

## Nature of the Active Component in a $\text{Fe}_2\text{O}_3\text{-MoO}_3$ Catalyst I. Study on the Catalyst Reduction and Oxidation\*

F. TRIFIRO', V. DE VECCHI, AND I. PASQUON

*From the Istituto di Chimica Industriale del Politecnico, Milano, Italy*

Received July 30, 1968

The reduction of a catalyst based on  $\text{Fe}_2\text{O}_3\text{-MoO}_3$  with  $\text{N}_2/\text{H}_2$  and  $\text{N}_2/\text{NH}_3$  as reducing mixtures has been studied by a thermogravimetric method. At the same time the products formed have been analyzed by IR and X-ray powder-diffraction techniques. The initial catalyst contains ferric molybdate, which is the first that is reduced (to ferrous molybdate), and molybdic anhydride, which is reduced to  $\text{MoO}_2$ . Thermal treatments of the catalyst at a temperature higher than  $600^\circ\text{C}$  in air flow can lead to irreversible phenomena, such as sintering. Oxidations, following a reduction, must be carried out at  $T > 450^\circ\text{C}$  to ensure a total reoxidation of ferrous molybdate, and with an oxidizing mixture containing a low percentage of  $\text{O}_2$  (e.g., 5%) in nitrogen, to avoid catalyst decomposition due to local overheating. The re-oxidation rate is higher than the rate of reduction.

The behavior of ferric molybdate during reduction suggests that the combined iron oxide of the catalyst plays a determining role in the oxidation processes of organic molecules carried out in the presence of catalysts based on  $\text{Fe}_2\text{O}_3\text{-MoO}_3$ .

### INTRODUCTION

Molybdic anhydride is a very selective catalyst for the oxidation reactions of methanol to formaldehyde and of propylene to acrolein, but, due to its low activity, it is employed in a mixture with other oxides.

A mixed oxide  $\text{Bi}_2\text{O}_3\text{-MoO}_3$  at a ratio  $\text{Bi}/\text{Mo} = 1$  is a catalyst for the oxidation of propylene to acrolein (1), while a mixed oxide  $\text{Fe}_2\text{O}_3\text{-MoO}_3$  at a ratio  $\text{Fe}/\text{Mo} = 0.4$  is an industrial catalyst for the oxidation of methanol to formaldehyde (2). In the case of the catalyst based on mixed oxides Bi and Mo, two types of bismuth molybdates are present (3); however, it is unknown which is the catalytically active compound. According to Batist *et al.* (4) in this class of catalysts, the role of Bi is to facilitate removal of water from the surface, whereas that of molybdenum is to adsorb olefins. According to Boreskow *et al.* (5), iron molybdate is the active

component of the catalyst based on  $\text{Fe}_2\text{O}_3\text{-MoO}_3$ .

As to this last catalyst system, some authors (6) proposed that the oxidation reactions taking place on its surface occur through an oxireductive (redox) mechanism. In this mechanism, however, the chemical nature of the so-called Cat-Red (reduced catalyst) has not been determined: the knowledge of it may help us to define what is the role of the two metals in the catalytic system.

In order to get information on the chemical nature of Cat-Red, we studied the rate of reduction of an industrial catalyst based on  $\text{Fe}_2\text{O}_3\text{-MoO}_3$  with an excess of  $\text{MoO}_3$  over the stoichiometric amount corresponding to iron molybdate. To this end, we simultaneously investigated the reduction rate and the nature of the products that form.

The reduction carried out by us is more drastic than the surface reduction the catalyst is subjected to during the oxidation reaction.

However, we feel that the nature of the

\* This work was sponsored by Consiglio Nazionale delle Ricerche, Italy.

species that form in the surface reduction of the catalyst is connected with that of the species that form in the tridimensional reduction.

### EXPERIMENTAL

Reactions of reduction and oxidation were carried out in an Adamel TH 59-2 thermobalance, which had been suitably modified for measurements in gaseous stream.

The inflow gas, after purification, was introduced to the upper part of the thermobalance to favor the contact between the solid and the gaseous phases.

Nitrogen and the mixtures N<sub>2</sub>-H<sub>2</sub> and N<sub>2</sub>-O<sub>2</sub> were dried by Mg perchlorate, whereas the N<sub>2</sub>-H<sub>2</sub> mixture was contacted with drops of anhydrous NaOH.

Caution was taken against the presence of oxygen in nitrogen and in the mixtures N<sub>2</sub>-H<sub>2</sub> by letting the gases pass over copper chips heated to 250°C.

Tests were carried out as follows:

(1) The catalyst was left standing at 540°C for 1½ hr under N<sub>2</sub> flow (50 l/hr). No weight loss is observed under these conditions.

(2) Temperature was adjusted to the desired value.

(3) Change of the flow and introduction of the reducing mixture (50 l/hr) were carried out.

In the case of oxidation tests, after a first reduction at 540°C by a mixture of N<sub>2</sub>-H<sub>2</sub> = 4, until a weight loss equal to 5% of the initial weight of the catalysts, the following method was adopted:

(1) The partially reduced catalyst was left standing at 540°C for about ½ hr under N<sub>2</sub> flow (50 l/hr).

(2) Temperature was adjusted to the desired oxidation temperature.

(3) Change of the flow and introduction of the oxidation mixture (50 l/hr) were carried out.

The examples reported in Figs. 1, 2, 3 have been corrected in the initial part by taking into account the effects of the different densities of the fed mixtures.

The amount of the corrections was established by blanks. The amount of Fe-Mo

used was 0.5 + 1 g; correspondingly measurements were performed with a sensitivity of about 2 ± 1 mg/mm. The actual sensitivity was measured every time for every run. The same flow rate was used for all gaseous mixtures in order to reduce the effect of the dynamic thrust, while fed gases were changed. It was actually observed that also the absolute effect of the dynamic thrust, in the field of rate of experimental flow, is minimum. IR spectra were recorded by the technique of KBr tablets, using a Perkin-Elmer infrared spectrometer. X-Ray diffraction spectra were recorded by Co K $\alpha$  radiation, using a Geiger-counter Philips spectrogoniometer.

The reagents used were as follows: Fe-Mo, an industrial catalyst with the composition MoO<sub>3</sub>, 82.5%; Fe<sub>2</sub>O<sub>3</sub>, 17.5% by weight; perforated cylindrical pellets,  $h = 4$  mm,  $\phi = 4$  mm, surface area = 7.2 m<sup>2</sup>/g; nitrogen, impurities < 5.5 ppm, supplied by SIO; hydrogen, impurities < 10 ppm, supplied by SIO; oxygen, 99.5%, supplied by SIO; ammonia, 99.9%; supplied by SIO.

### RESULTS

#### *Reduction Runs of the Catalyst*

Figure 1 shows the reduction runs of the catalyst in the thermobalance with mixtures nitrogen and hydrogen and nitrogen and ammonia at different temperatures. The percent weight loss vs. the initial weight is plotted on the ordinate; the time of standing at the reaction temperature on the abscissa.

The reduction runs were carried out at 350°C with a mixture of nitrogen and ammonia, the weight loss in the nitrogen and hydrogen stream being practically nil. In fact, runs carried out by heating the catalyst in the nitrogen and hydrogen stream with a heating rate of 150°C/hr showed that reduction starts at about 420°C.

The flow rate of the reduction mixture was brought to double its value and to half its value indicated for the runs reported in Fig. 1; in these runs, carried out with a nitrogen and hydrogen mixture, no variation of the weight loss rate in the

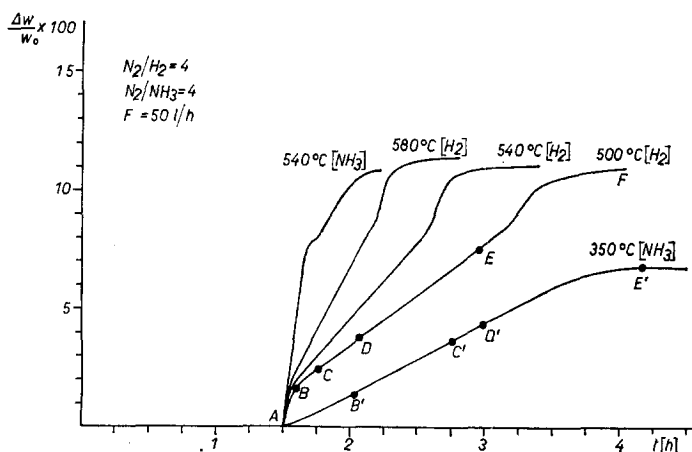


FIG. 1. Reduction of Fe-Mo catalyst with  $N_2/H_2$  and  $N_2/NH_3$  at various temperatures.

whole range of the curves of Fig. 1 was noticed. Runs were also performed with catalysts in granules of 30 + 60 mesh at 540°C and no variation of the weight loss rate of the catalyst was observed. Therefore, we may exclude for all three branches of the curves of Fig. 1 that the kinetics of the phenomenon is controlled by gas diffusion processes. Instead, all three branches of the reduction curve are influenced by the hydrogen concentration. The concentration of  $H_2$  was varied from 5% to 20%.

In the first part of the reduction curves, due to the non-steady-state conditions of concentration and buoyancy, it is difficult to draw reliable data. In the intermediate part (CE segment in Fig. 1) the weight loss rate is of first order with respect to hydrogen and in the last part of order higher than one.

We limited our reduction experiments to  $T < 600^\circ C$ , since at higher temperatures

the catalyst is subjected to sintering. We have seen that the apparent density of the catalyst maintained for about 1 hr at 650°C in air flow nearly doubles. These sintering phenomena are concomitant with sublimation of  $MoO_3$ . In the internal part of the cylinder of the catalyst white needles of  $MoO_3$  were found.

#### Reoxidation Runs

Figure 2 reports a set of reduction with  $N_2-H_2$ , oxidation with  $N_2-O_2$  (5%  $O_2$ ), and subsequent reduction of the catalyst with  $N_2-H_2$  carried out at 540°C. Under these conditions, the curve of the second reduction (RS portion) of the sample is almost the same as that corresponding to the first reduction (PQ portion).

The same figure also reports a set of results concerning oxidations carried out at three different temperatures on samples previously reduced at 540°C. It may be

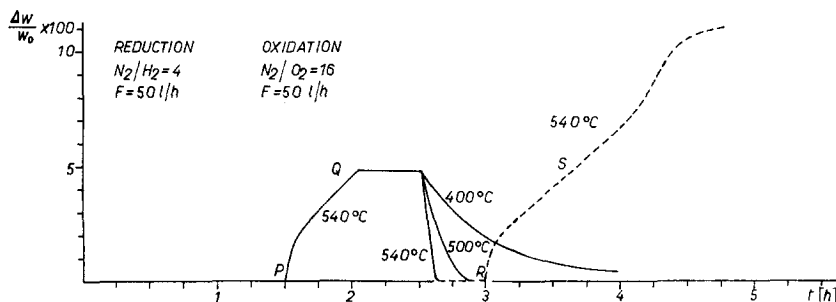


FIG. 2. Reduction and subsequent oxidation with  $N_2/O_2 = 16$  at different temperatures of Fe-Mo catalyst.

TABLE 1  
 X-RAY DATA (d) FOR DIFFERENT REDUCTION LEVELS

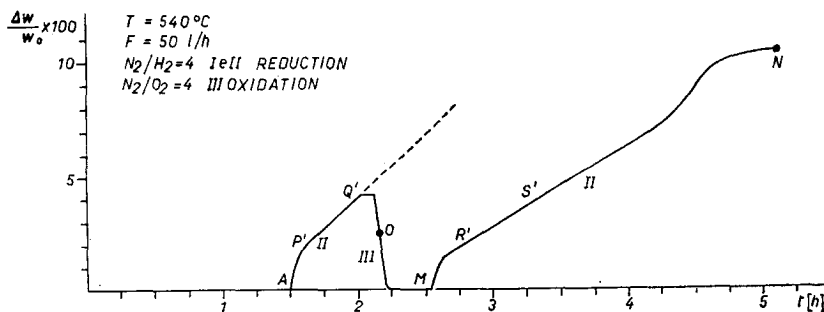
Point A starting sample	Point B red. with H <sub>2</sub>	Point B' red. with NH <sub>3</sub>	Point E' red. with NH <sub>3</sub>	Point D red. with H <sub>2</sub>	Point E red. with H <sub>2</sub>	Point F red. with H <sub>2</sub>
6.91 w	6.90 m	6.88 w	6.25 w	6.32 w	6.30 w	5.02 vw
6.30 vw	6.30 w	6.28 vw	3.52 vw	4.23 vw	4.73 vw	4.93 w
5.72 vw	4.72 vw	3.84 vw	3.42 vs	3.98 m	3.99 vw	4.80 vw
4.52 vw	3.97 vw	3.81 vw	3.16 w	3.95 m	3.85 vw	3.51 w
4.32 vw	3.79 s	3.79 w	2.78 vw	3.84 vw	3.75 vw	3.41 vs
4.07 w	3.45 s	3.45 w	2.74 vw	3.74 w	3.53 vw	2.76 vw
3.85 vs	3.39 w	3.39 vs	2.42 s	3.49 w	3.49 vw	2.51 vw
3.79 m	3.25 vs	3.24 s	2.40 m	3.39 vs	3.40 vs	2.44 m
3.55 vw	3.15 w	3.15 vw	2.10 vw	3.29 vw	3.29 vw	2.42 vs
3.46 s	2.77 vw	2.65 w	1.72 vw	3.15 w	3.16 w	2.40 s
3.25 vs	2.74 vw	2.41 vw	1.71 m	2.82 vw	2.77 vw	2.25 vw
3.20 vw	2.69 vw		1.69 vw	2.76 vw	2.74 vw	1.99 vw
2.95 vw	2.64 w			2.71 vw	2.66 vw	1.84 vw
2.83 vw	2.33 vw			2.66 w	2.42 s	1.72 m
2.70 vw	2.30 w			2.10 vw	2.40 w	1.70 m
2.65 vw	2.10 vw			1.94 vw	2.11 vw	1.69 w
2.62 vw	1.91 vw			1.72 vw	1.91 vw	1.55 vw
2.52 vw	1.84 vw			1.71 vw	1.72 w	
	1.73 vw				1.70 m	
	1.66 vw				1.69 w	
	1.62 vw				1.53 vw	
	1.59 vw				1.40 vw	
	1.56 vw					

observed that in the tests carried at 500° and 540°C the sample reaches its initial weight. This and the analogy between the PQ on RS lines allowed us to exclude weight loss by sublimation of the catalyst components.

Figure 3 reports a set of reductions with N<sub>2</sub>-H<sub>2</sub> oxidation with N<sub>2</sub>-O<sub>2</sub> (20% O<sub>2</sub>) and subsequent reduction with N<sub>2</sub>-H<sub>2</sub> carried out at 540°C. Under these conditions (that is, with a higher percent of O<sub>2</sub>) the subse-

quent reduction exhibits a far lower rate of weight loss (compare the slopes of segments R'S' and P'Q'). We have observed that after reduction and oxidation with N<sub>2</sub>-O<sub>2</sub> (O<sub>2</sub>, 20%), the catalyst samples presented black regions in the inner part of the small cylinder, which is an evidence of an irreversible phenomenon.

The data reported in Figs. 2 and 3 show that the oxidation rate is higher than the reduction rate with hydrogen, even when


 FIG. 3. Reduction, oxidation with N<sub>2</sub>/O<sub>2</sub> = 4, and subsequent reduction of Fe-Mo catalyst.

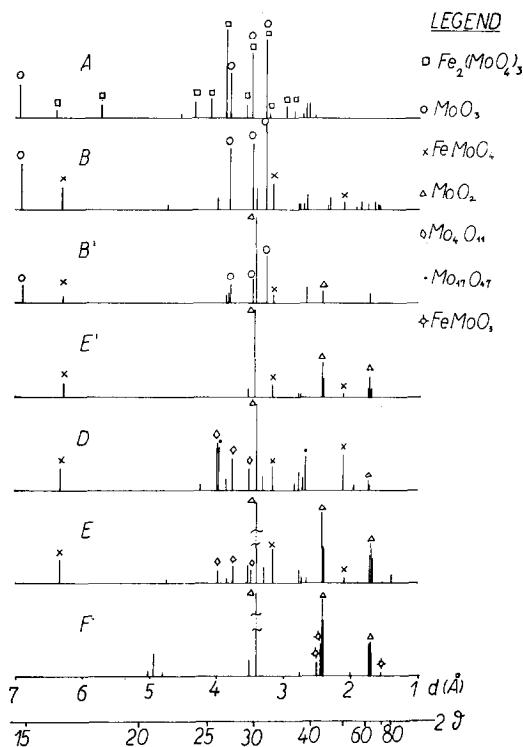


FIG. 4. X-Ray spectra at different hydrogen-nitrogen and ammonia-nitrogen reduction stages. See letters in Fig. 1.

a low concentration of  $O_2$  is used. The value of the rate of oxidation can be compared with that of reduction with ammonia.

#### X-Ray Analysis

Figure 4 and Table 1 report the data obtained from the X-ray analysis performed on the starting sample and on samples reduced at different levels, precisely in the corresponding points of the curve of Fig. 1.

The lines characteristic of  $MoO_3$  and ferric molybdate can be singled out in the spectrum of the starting catalyst (Fig. 4 A). The peaks at  $d = 3.25$  and  $3.46$  Å of  $MoO_3$  (7) are practically superimposed on the peaks at  $d = 3.237$  and  $3.46$  Å of ferric molybdate (5); due to this reason the intensity relations for these peaks are not respected.

In the spectrum of a sample reduced to point B of the curve of Fig. 1 the peaks corresponding to ferric molybdate are absent, the characteristic A peaks corresponding to ferrous molybdate (8) ( $d =$

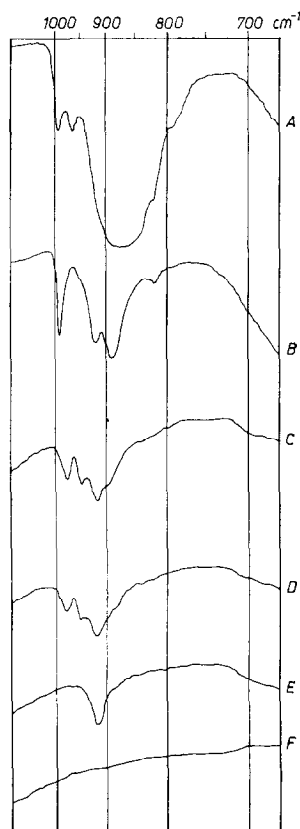


FIG. 5. IR Spectra at different hydrogen-nitrogen reduction stages ( $500^\circ C$ ). Spectra are marked with letters corresponding to those of Fig. 1.

6.3, 2.10, 3.14 Å) appear, and those of  $MoO_3$  are still present.

In the spectrum of the sample reduced to point D the bands of ferrous molybdate are present, as well as the bands corresponding to  $Mo_4O_{11}$ ,  $Mo_{17}O_{47}$  (7), and the very intense band of  $MoO_2$  at  $3.40$  Å. The spectrum of a sample reduced to point E reveals the peaks characteristic of ferrous molybdate and of  $MoO_2$ .

In the spectrum of a sample reduced to point F, the peaks corresponding to  $MoO_2$  (7) are still present, whereas that corresponding to ferrous molybdate is absent and new bands are found at  $d = 2.44$ ,  $2.51$ , and  $1.555$  Å (7), corresponding to  $FeMoO_3$ . We have also reported the X-ray data on the catalyst reduced with the  $N_2-NH_3$  mixture at  $350^\circ$ . In a sample reduced at point B', we can see that the bands of  $Fe_2(MoO_4)_3$  disappear and the bands of  $FeMoO_4$  appears, whereas the bands of

MoO<sub>3</sub> are still present. In the sample reduced at point E', where weight loss was not detectable any longer, the bands of FeMoO<sub>4</sub> and of MoO<sub>2</sub> are present.

### Infrared Spectra

Figures 5, 6, and 7 show the IR spectra of the catalyst at different reduction steps, precisely at the points of the curves of Figs. 1 and 3. The corresponding points are marked by the same letters in Figs. 1, 3, 5, 6, 7. At the end of the AB portion of Fig. 1 the band at 960 cm<sup>-1</sup> disappears in connection with the disappearance, in the X-ray spectra, of the characteristic lines of ferric molybdate. We can attribute this band at 960 cm<sup>-1</sup> to ferric molybdate. Already in the initial part of the BE portion—point C—the band at 985 cm<sup>-1</sup> of molybdic anhydride disappears, and new bands appear at 970 and 940 cm<sup>-1</sup>, probably due to Mo<sub>4</sub>O<sub>11</sub> or Mo<sub>17</sub>O<sub>47</sub>, which are nonstoichiometric Mo oxides with an O:Mo ratio ranging from 2 to 3. In the EF portion, the band at 915 cm<sup>-1</sup> that is present from step B disappears, and simultaneously the characteristic bands of ferrous molybdate disappear in the X-ray spectra. We can attribute the band at 915 cm<sup>-1</sup> to ferrous molybdate.

The order of disappearance of the bands in the reduction with ammonia at 550°C

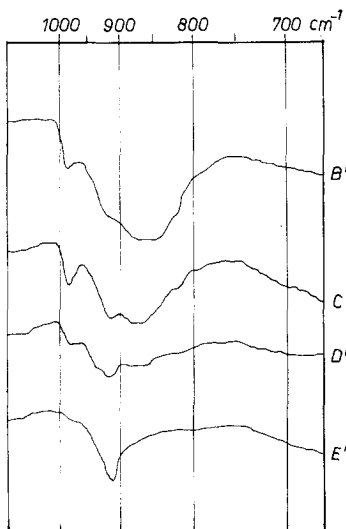


FIG. 6. IR Spectra at different ammonia-nitrogen reduction stages (350°C). See letters in Fig. 1.

is the same as in the reduction with hydrogen. Figure 6 shows the IR spectra of samples reduced with ammonia at a lower temperature (350°C). The order of disappearance of the bands is identical with that observed in the runs carried out at a high temperature; however, in this case the disappearance of the bands corresponding to MoO<sub>3</sub> is slower and more gradual than noticed at higher temperatures.

Figure 7 shows the IR spectra of a catalyst hydrogen reduced at 540° and reoxidized with oxygen at 20% and subsequently reduced (Fig. 3). Spectrum M was run on a sample drawn from the external part of the oxidized catalyst, spectrum M' on a sample drawn from the black inner part. Spectrum N corresponds to the sample at the end of the second reduction, i.e., when no weight loss is sensibly recognizable. It is still possible to see the band at 985 cm<sup>-1</sup> of MoO<sub>3</sub>.

Figure 7 also reports (letter O) the IR spectrum of a sample reduced at the temperature of 540°C, reoxidized at the same temperature, and stopped at half curve of

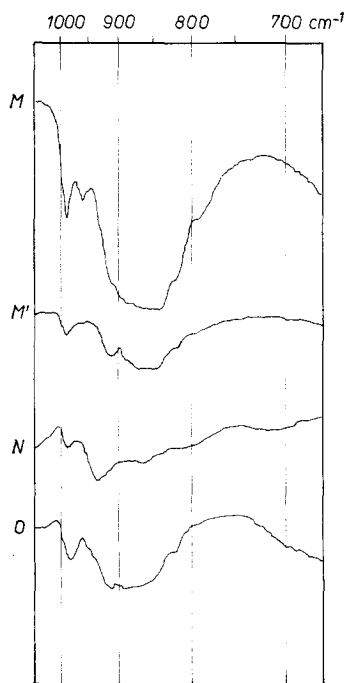


FIG. 7. IR Spectra concerning test in Fig. 3. M' is the spectrum of the black inner part of the oxidized catalyst.

oxidation. As may be seen, the band of  $\text{MoO}_3$  (at  $985\text{ cm}^{-1}$ ) and that of ferrous molybdate (at  $915\text{ cm}^{-1}$ ) are still present, whereas the band at  $960\text{ cm}^{-1}$  of ferric molybdate is absent. Therefore, in the oxidation reaction of a reduced catalyst, ferrous molybdate is the last to be oxidized.

## DISCUSSION

### *Nature of the Reduction Products*

As reported in Fig. 1, the high-temperature reduction with hydrogen of an industrial catalyst based on mixed oxides of iron and molybdenum exhibits three subsequent steps with different rates. When trying to interpret the reduction steps we have excluded the influence exerted by the weight loss originating from sublimation phenomena, according to the experiments reported in Figs. 2 and 3, where the catalyst after reoxidation retains all its initial weight.

X-Ray and IR analyses reveal that the catalyst reduction process is accomplished in three successive steps. In the first step (e.g., portion AB of Fig. 1) ferric molybdate is reduced to  $\text{FeMoO}_4$ , then (e.g., portion BE of Fig. 1) molybdic anhydride is reduced to  $\text{MoO}_2$  and in the last step (e.g., portion EF of Fig. 1) ferrous molybdate is reduced most probably only to  $\text{FeMoO}_3$ .

Table 2 reports the weight losses calculated for the reduction of the above-mentioned compounds and the experimen-

tal losses drawn as an average of the curve of Fig. 1.

The weight loss calculated by reduction of the whole iron to bivalent and of molybdenum to tetravalent is not very different from the experimental one, thus proving that considerable reductions to lower valencies than the supposed ones do not exist.

There are, however, discrepancies between the weight losses of the single compounds, whereas they seem to be reduced along the curves of Fig. 1 and the calculated weight losses. The weight loss in the intermediate portion where—as we stated—reduction of free  $\text{MoO}_3$  occurs, is far higher than that of the calculated value by considering that the whole iron reacted to give iron molybdate. This might be explained by supposing that also ferrous molybdate may be reduced along the intermediate portion.

The order of the subsequent reduction of the compounds present in the catalyst is identical in the low-temperature reduction with ammonia, under conditions near those at which the catalyst operated in industrial reactions. Therefore, we may conclude that, in the catalyst system based on mixed oxides of iron and molybdenum,  $\text{Fe}_2(\text{MoO}_4)_3$ , which is considered by some authors (5) as the active component for the oxidation of  $\text{CH}_3\text{OH}$  to  $\text{CH}_2\text{O}$ , is also the most easily reducible.

It was observed that in the reduction

TABLE 2  
WEIGHT LOSS OF A Fe-MO CATALYST DUE TO REDUCTION ( $\text{MoO}_3$  82.5%,  $\text{Fe}_2\text{O}_3$  17.5%)

	Experimental weight loss	Calculated weight loss		
	(avg from tests at 3 temps.)			
	Avg wt loss (%)		Comp. (%)	Wt loss reduction (% tot)
1st portion <sup>a</sup>	2.22	$\text{Fe}_2\text{O}_3$ as $\text{Fe}_2(\text{MoO}_4)_3$ <sup>d</sup>	17.5	1.75
2nd portion <sup>b</sup>	5.33	$\text{MoO}_3$ excess <sup>e</sup>	35.2	3.95
3rd portion <sup>c</sup>	2.75	$\text{MoO}_3$ as $\text{Fe}_2(\text{MoO}_4)_3$ <sup>e</sup>	47.3	5.25
Total	10.30		100.0	10.95

<sup>a</sup> E.g., AB segment, Fig. 1.

<sup>b</sup> E.g., BE segment, Fig. 1.

<sup>c</sup> E.g., EF segment, Fig. 1.

<sup>d</sup>  $\text{Fe}_2\text{O}_3 \rightarrow 2\text{FeO} + \frac{1}{2}\text{O}_2$

<sup>e</sup>  $\text{MoO}_3 \rightarrow \text{MoO}_2 + \frac{1}{2}\text{O}_2$

runs with N<sub>2</sub>-H<sub>2</sub> at a high temperature (e.g., 500°C), the X-ray and IR bands characteristic of MoO<sub>3</sub> disappear before the total MoO<sub>3</sub> is reduced to MoO<sub>2</sub> and that the nonstoichiometric oxides, Mo<sub>4</sub>O<sub>11</sub>, Mo<sub>17</sub>O<sub>41</sub>, are formed. The new bands that appear at 940 and 970 cm<sup>-1</sup> in the IR spectra of the partially reduced samples may be attributed to one of these oxides (see Figs. 5 C and D).

In the reduction with NH<sub>3</sub> at 350°C, the IR band at 985 cm<sup>-1</sup> corresponding to MoO<sub>3</sub> is present until a very advanced degree of reduction of MoO<sub>3</sub> to MoO<sub>2</sub>. Moreover, in this case, the new bands at 940 and 970 cm<sup>-1</sup> and the X-ray bands corresponding to Mo<sub>4</sub>O<sub>11</sub> and Mo<sub>17</sub>O<sub>47</sub> are not observed.

This different behavior may be attributed to the mobility of lattice oxygen. At high temperatures, cooperation phenomena between bulk and surface take place, due to the mobility of lattice oxygen. This phenomenon might be connected with a reaction between the surface-reduced oxide and the unreduced oxide in the bulk, to give nonstoichiometric oxides.

At lower temperatures, MoO<sub>3</sub> reduces layer by layer without cooperation of the reduced surface with the inner part of the catalyst.

#### *Reactivity of the Components of the System Fe<sub>2</sub>O<sub>3</sub>-MoO<sub>3</sub>*

The order of the subsequent reduction of the three compounds of hexavalent molybdenum, Fe<sub>2</sub>(MoO<sub>4</sub>)<sub>3</sub>, MoO<sub>3</sub>, FeMoO<sub>4</sub>, is connected with the reactivity of their surface in the reduction reaction and therefore with a certain lability of lattice oxygen. The lower reactivity of ferrous molybdate is also shown by the nonreactivity in the reduction with ammonia at low temperature.

The slow step of the reduction rate of the three compounds is not gas diffusion since the rate of reduction is practically independent of the flow rate and of the size of the pellets. The reduction rates for all three compounds depend on the hydrogen concentration. It is impossible to attribute the order of the reduction rate of ferric

molybdate with respect to hydrogen, since the conditions are not steady state; as calculated approximately, the activation energy is lower than 10 kcal/mole. The reduction rate of MoO<sub>3</sub> is of first order with respect to hydrogen and has an apparent activation energy of about 14 kcal/mole. The reduction rate of ferrous molybdate has an order higher than one with respect to H<sub>2</sub> and an apparent activation energy of about 18 kcal/mole. We can observe that this last value, although approximate, is higher than that corresponding to the more reactive compound.

#### *Irreversibility Phenomena in the Oxireductive Cycles*

As may be seen from Figs. 3 and 7, irreversibility phenomena take place on performing cycles of reduction, oxidation, and subsequent reduction, if high concentrations of oxygen are used for the oxidation runs.

Irreversibility phenomena exhibit the following features: a lower rate in the second reduction shown by the catalytic system, especially in the intermediate portion; after reoxidation, the presence of dark regions in the inner part of the small cylinder of catalyst, which show by IR only the bands of MoO<sub>3</sub> and of ferrous molybdate; and the presence of the bands of MoO<sub>3</sub> in the subsequent reduction of the catalyst, in the flattening region of the reduction curve, that is, where the weight loss was not detectable any longer. This suggests that molybdic anhydride stays inside the granules, owing to decomposition phenomena of oxides originating from local overheating.

These irreversibility effects must be taken into account in the thermal treatment or in the activation under vacuum with subsequent reoxidation of the reduced catalyst.

These phenomena may also occur during a catalytic reaction, if high-temperature spots exist; these last not only lead to a decrease in the activity, but above all to a decrease in the selectivity due to the chemical modifications the catalyst had to undergo. Therefore, the thermal conduc-



tivity of the granules may have a considerable importance in avoiding such irreversibility phenomena.

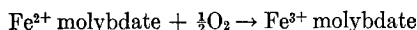
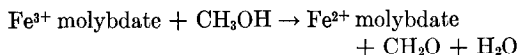
### Redox Mechanism

The redox mechanism in the oxidation reaction with catalysts of the type examined by us was proposed by Jirů and co-workers (6) for the oxidation of  $\text{CH}_3\text{OH}$  to  $\text{CH}_2\text{O}$ .

As to the catalytic system,  $\text{Fe}_2\text{O}_3\text{-MoO}_3$ , some authors have stated that the most active and selective component is iron molybdate (5).

In this work we have found that iron molybdate is the first component of the system  $\text{Fe}_2\text{O}_3\text{-MoO}_3$  that is reduced to give ferrous molybdate.

If we assume that a parallelism exists between the bulk reduction with  $\text{H}_2$  or  $\text{NH}_3$  and the stage of surface reduction of the catalyst during the catalytic reaction, typical of redox mechanism, we can put forth a chemical representation for this mechanism:



From this mechanism we may conclude that the role of iron in ferric molybdate as an oxidation catalyst is to transfer water and oxygen between the catalyst surface and the gas phase.

### CONCLUSIONS

(1) In the catalytic system  $\text{Fe}_2\text{O}_3\text{-MoO}_3$ , ferric molybdate is the most reactive com-

ponent in the reduction, between  $350^\circ$  and  $580^\circ\text{C}$ , with ammonia and hydrogen.

(2) The product of the reduction of ferric molybdate is ferrous molybdate. Ferrous molybdate presents a lower oxidation rate than  $\text{MoO}_2$ .

(3) Thermal treatments of the catalyst might be carried out at  $T < 600$  in order to avoid sintering of the catalyst and at  $T > 400^\circ\text{C}$  to guarantee the complete oxidation of ferrous molybdate.

(4) After reduction of the catalyst, a further oxidation with a low concentration of oxygen is required to avoid creating an irreversible modification.

(5) The iron in ferric molybdate seems to act as the transfer agent of oxygen and water between the surface and the gas phase.

### REFERENCES

1. BELGIAN PATENT 571200 (13/9/1958).
2. ADKINS, H., AND PETERSON, W. R., *J. Am. Chem. Soc.* **53**, 1512 (1931).
3. BLEYENBERG, A. C. A. M., LIPPENS, B. C., AND SCHUIT, G. C. A., *J. Catalysis* **4**, 581 (1965).
4. BATIST, PH., LIPPENS, B. C., AND SCHUIT, G. C. A., *J. Catalysis* **5**, 55 (1966).
5. BORESKOV, G. K., KOLOVERTNOV, G. D., KEFELI, G. L. M., PLYASOVA, L. M., KARAKCHIEV, L. G., MASTIKIN, V. N., POPOV, B. I., DZISKO, V. A., AND TARASOVA, D. V., *Kinetika i Kataliz* **7**, 144 (1966).
6. JIRŮ, P., WICHTERLOVA, B., AND TICHY, J., *Proc. Intern. Congr. Catalysis, 3rd, Amsterdam 1964* **1**, 199-213.
7. "Index to the Powder Diffraction File." American Society For Testing Materials, 1967.
8. JÄGER, W., RAHMEL, A., AND BECKER, K., *Arch. Eisenhüttenwes.* **30**, 435 (1959).